Colloid Polym Sci 277:388–393 (1999)

SHORT COMMUNICATION

K. Sekine

Finite-element calculations for dielectric relaxation of one-sphere systems in a parallel-electrode measuring cell

Received: 15 July 1998
Accepted in revised form: 5 November 1998

K. Sekine
School of Health Sciences
Faculty of Medicine
Kanazawa University
5-11-80 Kodatsuno
Kanazawa, Ishikawa 920-0942, Japan
Tel: +81-76-2652586; Fax: +81-76-2344360
e-mail: sekine@kenroku.kanazawa-u.ac.jp

Abstract Using the finite-element method (FEM), the frequency dependence of conductivity and relative permittivity was calculated for a heterogeneous specimen in which a sphere was placed in a medium. The FEM calculations were made for the whole system in which the specimen was located in a measuring cell comprising two parallel electrodes and a spacer with a cylindrical sample cavity, as in practical measurements. Values of the conductivity and the permittivity of the sphere and the medium were chosen so as to simulate specimens of water-in-nitrobenzene (W/N) and oil-in-water (O/W) types. When the volume ratio of the sphere to the sample cavity p was below 0.1, the frequency dependence of conductivity and permittivity was in good agreement with that described by Wagner's theory for both the W/N and O/W specimens. When p was greater than 0.1, deviations from Wagner's theory were found for limiting values of the conductivity and permittivity at low and high frequencies for both the W/N and O/W specimens, and for the relaxation time for the W/N specimens.

Key words Dielectric relaxation – Finite-element method – Heterogeneous system – Interfacial polarization – Simulation

Introduction

Colloidal systems show dielectric relaxation from several origins such as motion of polar groups of constituent molecules, motion of counterions at charged surfaces and accumulation of ions at interfaces under external electric fields [1–5]. Measuring the specimens using well-designed apparatuses and analyzing the observed data by appropriate theories provide valuable information on molecular motion, structure and electrical properties of the colloidal systems.

In practice, several types of measuring cells are used in frequency-domain dielectric spectroscopy in the radio-frequency region (below 10^7 Hz). One of the simplest measuring cells comprises a pair of parallel-plate electrodes and a plate spacer in which a hole is bored to form a sample cavity. Measuring cells of this type were originally designed for measurements on suspensions of biological cells and on homogeneous solutions [6]. Asami and coworkers [7–9] used similar measuring cells for measurements of a single millimeter-sized sphere immersed in a medium, to make clear the relation between the structure of the particles and the dielectric spectra. These experimental studies serve as the basis of structural analysis using dielectric spectroscopy in colloid science and biology. Asami and Zhao [10] developed this technique for measurements of a single sub-millimeter sized sphere using a three-terminal chamber. As a more sophisticated design, the electrodes were attached to rheometers to investigate in situ the deformation of droplets in concentrated emulsions [11] and the change in the aggregate structure in a suspension under shearing flow [12]. The scanning dielectric microscope comprises a fixed plate electrode and a movable guarded pin electrode [13–15]. A vibrating electrode was used in simultaneous monitoring

of viscoelastic and dielectric properties of curing epoxy resins [16].

For modification of the measuring cells, the most important problem is that it is difficult to assess the artifacts in the measurements [6, 17] from the design drawings. In the present study, a numerical method based on the finite-element method (FEM) [18, 19] for the assessment of the artifacts is developed. As an example, the system studied experimentally by Asami and coworkers [7–9] containing a single millimeter-sized sphere in a parallel-plate-type measuring cell is simulated, because this system provides important information irrespective of its simple geometry. To simplify the problem, the sphere is assumed to be homogeneous and to have no fixed charges in its interior and at its surface. Attention is paid to the effects of the size of the sphere. The artifacts caused by these effects are characterized by comparing the results of the simulation with Wagner's theory, which describes the dielectric properties of dilute suspensions of spheres [1–5].

Theory and methods of calculation

Wagner's theory

Electromagnetic phenomena in materials are described by the Maxwell equations. Since we are concerned with dielectric behavior at frequencies below 10^7 Hz, quasi-static electric fields can be assumed. In such a case, Laplace's equation is applicable to a system without space charge [20, 21].

$$\mathrm{div}(\kappa^* \,\mathrm{grad}\,\phi) = 0 \ , \tag{1}$$

where ϕ denotes the electric potential and κ^* the complex conductivity. The complex conductivity κ^* is defined by the relation

$$\kappa^* = \kappa' + i\kappa'' = \kappa + i\omega\varepsilon_0\varepsilon \ , \tag{2}$$

using an imaginary unit i, a real part κ' and an imaginary part κ'', with κ' and κ'' being represented by the conductivity κ, the circular frequency of the electric fields ω, the permittivity of vacuum ε_0 and the relative permittivity ε.

Wagner's theory [2–5] is derived on the basis of Eq. (1) by calculating analytically the equivalent dipole moment of a spherical region in suspensions of spheres under the following assumptions:

1. The suspensions are placed in uniform external electric fields.
2. Electrical interactions between the spheres can be neglected.
3. Interfacial phenomena at the surface of the spheres can be described simply by the boundary conditions

$$\phi_1 = \phi_2 \ , \tag{3}$$

$$\kappa_1^* \mathbf{E}_1 \mathbf{n}_1 + \kappa_2^* \mathbf{E}_2 \mathbf{n}_2 = 0 \ , \tag{4}$$

where subscripts 1 and 2 denote the sphere and the medium, respectively, $\mathbf{n}$ is the unit vector normal to the surface and $\mathbf{E} = -\mathrm{grad}\,\phi$. From this theory, the complex conductivity $\kappa^*_{\mathrm{s,W_{ag}}}$ of the suspension is given by the relation

$$\kappa^*_{\mathrm{s,W_{ag}}} = \kappa_2^* \frac{(2\kappa_2^* + \kappa_1^*) - 2p(\kappa_2^* - \kappa_1^*)}{(2\kappa_2^* + \kappa_1^*) + p(\kappa_2^* - \kappa_1^*)} \ , \tag{5}$$

where p is the volume fraction of the suspension. Irrespective of the simplicity of the derivation, it has been shown experimentally that Wagner's theory is applicable to suspensions of large spheres without fixed charges when p is less than 0.1 [2, 4, 5].

Numerical analysis using FEM

Model

To simplify the problem, the FEM calculations were made using a model that was symmetric with respect to the z-axis and also to the r-plane in cylindrical coordinates, as shown in Fig. 1. In this model, a spacer having thickness T and radius R_3 is sandwiched by two electrodes. A cylindrical sample cavity with radius R_2 is bored at the center of the spacer. The specimen is a heterogeneous system comprising a sphere with radius R_1 and a medium. The sphere is located at the center of the sample cavity.

The FEM calculations were carried out on the basis of Eq. (1). Because of the axisymmetric arrangement of the model, Eq. (1) is represented in cylindrical coordinates:

$$\frac{\partial}{\partial r}\left(r\kappa^* \frac{\partial \phi}{\partial r}\right) + \frac{\partial}{\partial z}\left(r\kappa^* \frac{\partial \phi}{\partial z}\right) = 0 \ , \tag{6}$$

where r and z denote the radial and axial coordinate, respectively.

It was assumed that Eqs. (3) and (4) held at the sphere-medium interface. Similar conditions were

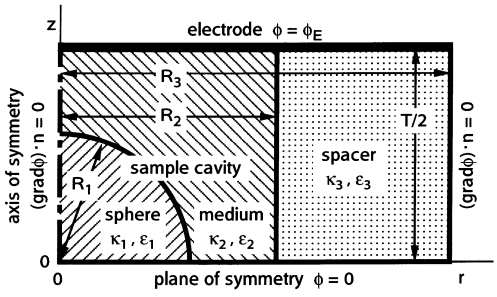

Fig. 1 The model used in the finite-element method (FEM) calculations for the one-sphere systems

assumed at the medium-spacer interface. The following conditions were enforced upon ϕ and $\mathbf{E}$ at the outer surface of the model:

1. $\phi = \phi_E$ when $z = T/2$.
2. $\phi = 0$ when $z = 0$.
3. $\mathbf{E}\,\mathbf{n} = 0$ when $r = 0$ or $r = R_3$.

FEM calculation

In the FEM calculations, the region in question was subdivided into triangular elements, in which ϕ was a linear function of r and z, and κ^* was a constant. Using the values of ϕ obtained from the calculations, the values of the surface density σ of charges accumulated at the interfaces were calculated from the following relation, which was derived on the basis of Eq. (4):

$$\sigma = -\varepsilon_0(\kappa_j^* \mathbf{E}_j\,\mathbf{n}_j + \kappa_k^*\,\mathbf{E}_k\,\mathbf{n}_k)\ , \tag{7}$$

where subscripts j and k represent the materials. The admittance Y of the whole region was calculated from the relation

$$Y = -\frac{I}{2\phi_E}\ , \tag{8}$$

where I was obtained by summing the current densities $\kappa^*\mathbf{E}\,\mathbf{n}$ over the whole electrode surface, $\kappa^*\mathbf{E}\,\mathbf{n}$ being obtained as the result of the FEM calculations.

The values of the parameters used in the FEM calculations are shown in Table 1. The radius R_1 of the sphere was changed from 0.5 to 4.6 mm to examine the effects of R_1 on the dielectric relaxations. The water-in-nitrobenzene (W/N) and the oil-in-water (O/W) systems simulate heterogeneous specimens of W/N structure and those of O/W structure, respectively. The values of κ and ε of the spacer are typical of insulating nonpolar materials [22].

Table 1 Parameter values used in the finite-element method (FEM) calculations for water-in-nitrobenzene (W/N) and water-in-oil (O/W) systems

Potential	$\phi_E = 0.5V$	
Geometry	R_1 is changed from 0.5 to 4.6 mm	
	$R_2 = 5$ mm	
	$R_3 = 15$ or 20 mm	
	$T/2 = 5$ mm	
Electric properties of materials		
W/N system		
Sphere	$\kappa_1 = 1$ mS m^{-1}	$\varepsilon_1 = 80$
Medium	$\kappa_2 = 0$	$\varepsilon_2 = 35$
Spacer	$\kappa_3 = 0$	$\varepsilon_3 = 2$
O/W system		
Sphere	$\kappa_1 = 0$ mS m^{-1}	$\varepsilon_1 = 2$
Medium	$\kappa_2 = 1$	$\varepsilon_2 = 80$
Spacer	$\kappa_3 = 0$	$\varepsilon_3 = 2$

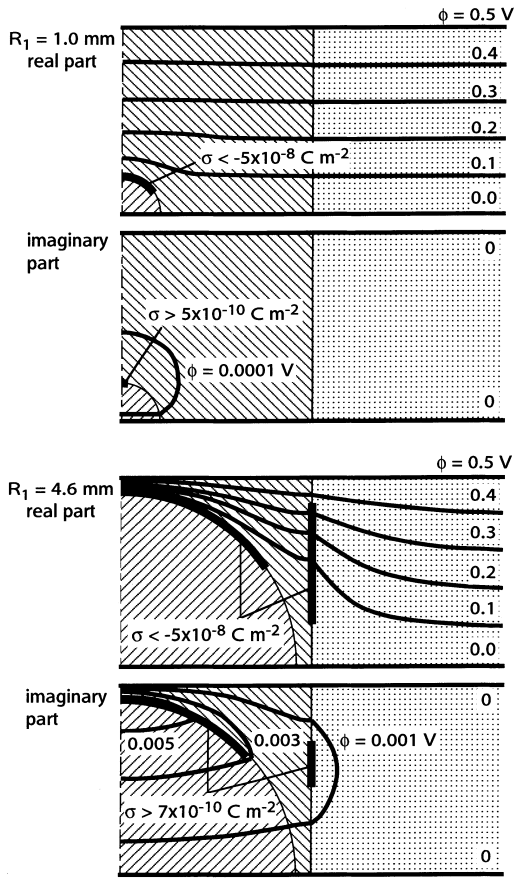

Fig. 2 Distribution of the electric potential ϕ and the charge (σ represents its surface density) in the measuring cell for water-in-nitrobenzene (W/N) systems at 10^3 Hz

Results and discussion

Distribution of potential and accumulated charge

The distribution of ϕ and σ in the W/N systems at 10^3 Hz is shown in Fig. 2. As seen from the figure, the charge accumulated at the sphere-medium interface modifies the distribution of ϕ in the measuring cell. When $R_1 = 1.0$ mm, effects of the accumulated charge are limited within the sphere and the medium. When $R_1 = 4.6$ mm, these effects extend into the spacer, producing accumulated charge at the medium-spacer interface and modifying the distribution of ϕ in the spacer. In addition, $\mathbf{E}$ in the sphere is nonuniform when $R_1 = 4.6$ mm.

Effective complex conductivity of the sample

The value of Y evaluated from Eq. (8) contains the contributions of the specimen and the spacer. If $\mathbf{E}$ in the spacer is uniform and parallel to the z-axis, these

contributions can be represented by a lumped circuit model comprising two admittance elements in parallel corresponding to the specimen and the spacer [17]; thus, Y is given by the relation

$$Y = \kappa^*_{s,FEM}\frac{\pi R_2^2}{T} + \kappa^*_3\frac{\pi(R_3^2 - R_2^2)}{T} \quad , \tag{9}$$

where $\kappa^*_{s,FEM}$ represents the effective complex conductivity of the specimen placed in the measuring cell and κ^*_s represents the complex conductivity of the spacer.

In the present study, Eq. (9) was used to evaluate $\kappa^*_{s,FEM}$. Although it may be unreasonable to apply Eq. (9) in large-R_1 regions as seen from Fig. 2, this treatment that is the same as that used in experimental studies is helpful to assess the artifacts produced by the increase in R_1. The frequency dependence of $\kappa^*_{s,FEM}$ obtained using mesh S46b listed in Table 2 is shown in Fig. 3.

Comparison with Debye-type relaxation

The dielectric relaxation with a single relaxation time is phenomenologically represented by the Debye formula

$$\kappa^* = \kappa_L + \frac{i\,\omega\,\tau\,(\kappa_H - \kappa_L)}{1 + i\omega\tau} + i\,\omega\,\varepsilon_0\,\varepsilon_H \quad , \tag{10}$$

$$(\varepsilon_L - \varepsilon_H)\,\varepsilon_0 = (\kappa_H - \kappa_L)\,\tau \quad , \tag{11}$$

where $\kappa_L, \kappa_H, \varepsilon_L$ and ε_H denote the limiting values of the conductivity and the relative permittivity at low (subscript L) and high (H) frequencies. The term τ denotes the relaxation time [1–5].

In order to examine if the dielectric relaxation calculated by FEM is simulated by the Debye formula, it was compared with the calculation from Eqs. (10) and (11). The results in a large-R_1 region are shown in Fig. 3. The solid lines calculated from Eqs. (10) and (11) with the most suitable values of $\kappa_L, \kappa_H, \varepsilon_L$ and ε_H are seen to be in good agreement with the frequency dependence of $\kappa^*_{s,FEM}$ of the O/W system. However, Fig. 4 clearly shows a significant difference between the Debye formula and the frequency dependence of $\kappa^*_{s,FEM}$ of the W/N system; the deviation increases with increasing R_1. This deviation indicates an apparent distribution of the relaxation times. In small-R_1 regions, the frequency dependence of $\kappa^*_{s,FEM}$ was found to agree with the Debye formula, in both the O/W and the W/N systems.

Since the accuracy of the FEM calculation depends on the size and the shape of each element and the arrangement of the elements, the calculations were performed using two or three different meshes to test

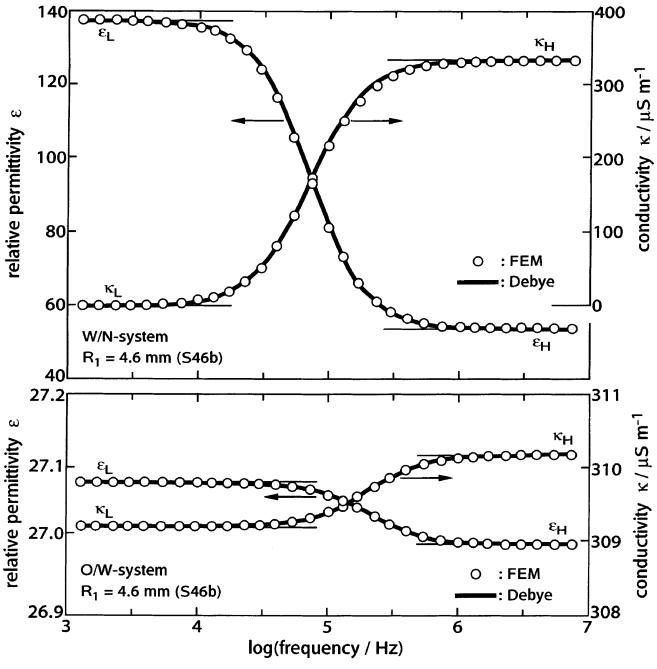

Fig. 3 Dielectric spectra of the one-sphere system in the parallel-plate-type measuring cell containing a sphere 4.6 mm in radius

Table 2 Characters of some of meshes used in the FEM calculations

Mesh	S10a	S10b	S10c	S46a	S46b
R_1/mm	1.0	1.0	1.0	4.6	4.6
R_3/mm	15	15	15	15	20
Number of nodes	420	454	704	737	831
Number of elements	781	845	1343	1387	1570
Limiting values of κ and ε of specimen[a]					
W/N system ($\kappa_L = 0$)					
κ_H	2.630	2.629	2.628	332.0	332.1
ε_L	35.566	35.566	35.565	137.39	137.39
ε_H	35.168	35.168	35.168	53.59	53.59
O/W system					
κ_L	992.05	992.05	992.04	309.4	309.2
κ_H	992.05	992.05	992.04	310.4	310.2
ε_L	79.388	79.388	79.387	27.09	27.08
ε_H	79.387	79.387	79.387	27.01	26.99

[a] Unit of κ is μS m^{-1}

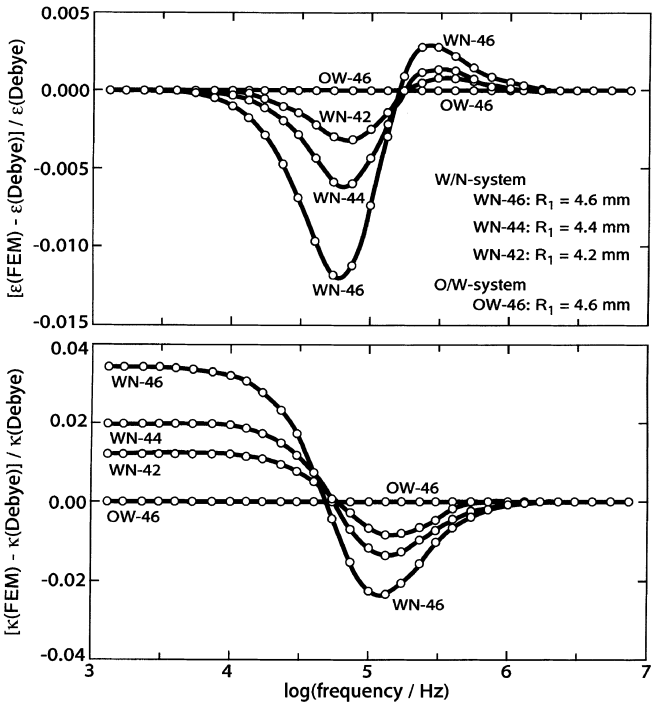

Fig. 4 Deviation of dielectric spectra of the one-sphere systems (FEM) from the Debye formula

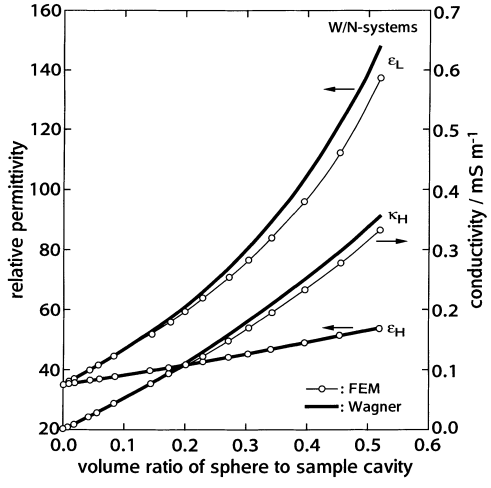

Fig. 5 Change in the limiting values of the conductivity κ_H, κ_L and the relative permittivity $\varepsilon_L, \varepsilon_H$ at low (subscript L) and high (H) frequencies with the volume ratio of the sphere to the sample cavity in the W/N systems

the validity of the calculations. The character of some meshes and the values of $\kappa_L, \kappa_H, \varepsilon_L$ and ε_H for $\kappa^*_{s,FEM}$ evaluated using these meshes are listed in Table 2. The agreement among these values indicates that the accuracy is satisfied in the calculations. Plots of $\kappa_L, \kappa_H, \varepsilon_L$

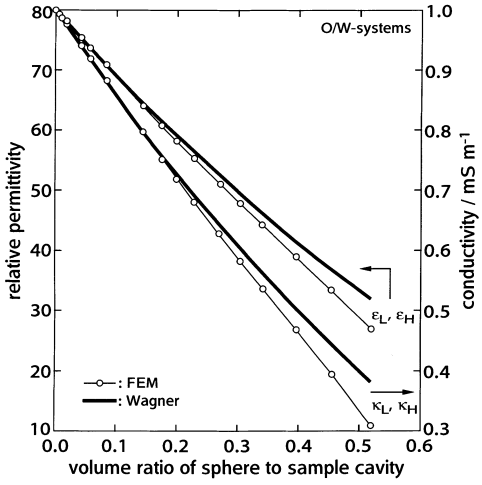

Fig. 6 Change in $\kappa_L, \kappa_H, \varepsilon_L$ and ε_H with the volume ratio of the sphere to the sample cavity in the oil-in-water (O/W) systems

and ε_H against the volume ratio of the sphere to the sample cavity are shown in Figs. 5 and 6.

Comparison with Wagner's theory

It is derived from Eq. (5) that $\kappa^*_{s,Wag}$ is represented by the Debye formula [1–5]. This behavior is parallel to that of $\kappa^*_{s,FEM}$ in the W/N systems in the small-R_1 regions and in the O/W systems, as described in the preceding section.

To compare the values $\kappa_L, \kappa_H, \varepsilon_L$ and ε_H for $\kappa^*_{s,FEM}$ with those for $\kappa^*_{s,Wag}, \kappa^*_{s,Wag}$ is calculated from Eq. (5) by taking the volume ratio of the sphere to the sample cavity to be p. The values of $\kappa_L, \kappa_H, \varepsilon_L$ and ε_H calculated for $\kappa^*_{s,Wag}$ (thick solid lines) and $\kappa^*_{s,FEM}$ (thin solid lines) are shown in Figs. 5 and 6. As seen from these figures, the values for $\kappa^*_{s,Wag}$ agree closely with those for $\kappa^*_{s,FEM}$ when the volume ratio of the sphere to the sample cavity is below 0.1: in high-volume-ratio regions, the values deviate from $\kappa^*_{s,FEM}$. The feature of the deviations is different among the parameters and is dependent on the electrical properties of the specimens, for example, the deviation in ε_H is very slight for the W/N systems.

Analysis based on Wagner's theory

The following relations are derived by substituting $\kappa_2 = 0$ or $\kappa_1 = 0$ into Eq. (5) [5].
If $\kappa_2 = 0$,

$$p = -\frac{1 - \varepsilon_L/\varepsilon_2}{2 + \varepsilon_L/\varepsilon_2} \quad , \tag{12}$$

and if $\kappa_1 = 0$,

$$p = \frac{2(1 - \kappa_L/\kappa_2)}{2 + \kappa_L/\kappa_2} \quad , \tag{13}$$

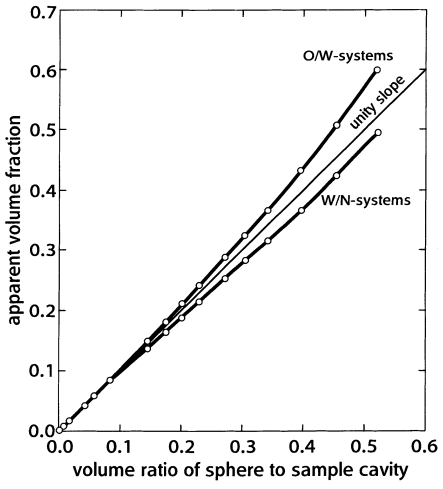

Fig. 7 Apparent volume fraction evaluated from the analysis of dielectric spectra of the one–sphere systems

where κ_2 and κ_1 denote the conductivities of the medium and the sphere, respectively, and ε_2 is the relative permittivity of the medium. Using the values of ε_L and κ_L for $\kappa^*_{s,FEM}$, the apparent volume fraction p_{app} was obtained from Eqs. (12) and (13), and is plotted against the real volume ratio of the sphere to the sample cavity p_{real} in Fig. 7.

As seen from Fig. 7, the values of p_{app} agree closely with those of p_{real} when p_{real} is less than 0.1. This result supports the validity of the choice of the sphere-cavity volume ratio in the model as p in Eq. (5), made in the preceding section. When p_{real} is greater than 0.1, p_{app} is less than p_{real} in the W/N systems and p_{app} is greater than p_{real} in the O/W systems. The behavior of p_{app} in the O/W systems is consistent with experimental observations by Asami and Irimajiri [8]. This supports the use of the FEM analysis in the present study.

Conclusion

The present study shows that FEM calculations of the dielectric relaxation can be practiced with the required accuracy. This suggests that the procedure in this study can be extended to various types of measuring cells by changing the geometry of the model. Effects of the interfacial phenomena can be investigated using more complicated boundary conditions and/or Poisson's equation in place of Eq. (1).

The dielectric properties of the one-sphere systems in the parallel-plate-type measuring cell are shown to be described by Wagner's theory when the volume ratio of the sphere to the sample cavity sphere is below 0.1. This result is not self-evident because Wagner's theory and the method used in this study are derived from different ideas. The validity of the choice of the sphere-cavity volume ratio in the one-sphere system as the volume fraction in Wagner's theory is not proved theoretically at this stage.

An increase in the size of the sphere causes several kinds of deviation from Wagner's theory, such as the distribution of relaxation times, and the deviation in the limiting values of the conductivity and the permittivity at low and high frequencies. These effects are dependent on the electrical properties of the specimen. This suggests that the artifacts should be assessed using appropriate standard materials in experimental studies.

Acknowledgements I thank K. Asami, Institute for Chemical Research, Kyoto University, for helpful advice.

References

1. Sjöblom J, Gestblom B (1992) In: Friberg SE, Lindman B (eds) Organized solutions. Dekker, New York, pp 193–219
2. Takashima S (1989) Electrical properties of biopolymers and membranes. Hilger, Bristol
3. Clausse M (1983) In: Becher P (ed) Encyclopedia of emulsion technology, vol 1. Dekker, New York, pp 481–715
4. Dukhin SS (1971) In: Matijevič E (ed) Surface and colloid science, vol 3. Wiley, New York, pp 83–165
5. Hanai T (1968) In: Sherman P (ed) Emulsion science. Academic Press, London, pp 353–478
6. Schwan HP (1963) In: Nastuk WL (ed) Physical techniques in biological research, vol 6(B). Academic Press, New York, pp 323–407
7. Asami K, Irimajiri A (1984) Biochim Biophys Acta 769:370–376
8. Asami K, Irimajiri A (1985) Bull Inst Chem Res Kyoto Univ 63:259–275
9. Asami K, Irimajiri A, Hanai T (1989) Bull Inst Chem Res Kyoto Univ 67:207–216
10. Asami K, Zhao KS (1994) Colloid Polym Sci 272:64–71
11. Adachi K, Fukui F, Kotaka T (1994) Langmuir 10:126–130
12. Genz U, Helsen JA, Mewis J (1994) J Colloid Interface Sci 165:212–220
13. Asami K (1994) Meas Sci Technol 5:589–592
14. Asami K (1995) Colloid Polym Sci 273:1095–1097
15. Asami K (1998) Colloid Polym Sci 276:373–378
16. Binder B, Schmid FS, Elsner P, Busse G (1993) Colloid Polym Sci 271:22–29
17. Smith G, Duffy AP, Shen J, Oliff CJ (1995) J Pharm Sci 84:1029–1044
18. Zienkiewicz OC (1977) The finite element method, 3rd edn. McGraw-Hill, London
19. Johnson C (1987) Numerical solution of partial differential equations by the finite element method. Cambridge University Press, Cambridge
20. Stratton JA (1941) Electromagnetic theory. McGraw-Hill, New York
21. Schwab AJ (1988) Field theory concepts. Springer, Berlin Heidelberg, New York
22. Laboratory for Insulation Research, Massachusetts Institute of Technology (1995) In: von Hippel A (ed) Dielectric materials and applications, 2nd edn. Artech House, Boston, pp 291–433